Royal Norwegian Council
for Scientific and Industrial Research
(NTNF)

NORSAR

NORSAR Scientific Report No. 1-87/88

Semiannual Technical Summary

1 April — 30 September 1987

L.B. Loughran (ed.)

Kjeller, December 1987

APPROVED FOR PUBLIC RELEASE, DISTRIBUTION UNLIMITED

VII.3 False alarm statistics and threshold determination for regional event detection

In order to improve the event detection performance during automatic processing of regional array data, the detection thresholds for the different beams need to be closely examined. In this context, several factors should be considered:

i) We wish to make the detection process as sensitive as possible with emphasis on small events, i.e., we want to operate on a low threshold.

ii) We need to specify how many false alarms per time unit can be accepted; e.g., operation of the NORSAR array has shown that false alarm rates of up to 50 % are acceptable.

iii) Too many false alarms will cause the phase association algorithm to produce fictitious events.

iv) The number of false alarms increases with the number of beams. In an extended beam set, we should only include the beams that improve the detectability without significantly increasing the number of false alarms.

In this study we have attempted to determine the thresholds for a large beam set from false alarm considerations. The procedure has been as follows:

1) Based on previous studies (Kværna and Mykkeltveit, 1986) and the NORSAR staff's experience with processing of regional array data (RONAPP), define the filter bands that appear most appropriate for regional event detection. The resulting twelve filters are given in Table VII.3.1.

2) For each filter band, find the best array sub-geometry and the corresponding steering delays for coherent beamforming. For detection of P-waves we have attempted to have maximum 3 decibels signal loss due to missteering. For coherent beam detection of S-waves, we have also applied the 3 dB criterion. The resulting P-wave beam deployment spanned the velocity space from 6.0 km/s to infinity, whereas the velocity space from about 3.8 km/s to 5.3 km/s was spanned by the S-beams. This resulted in 72 P-beams and 132 S-beams.

3) For each filter band, find the best array sub-geometry for incoherent beamforming of the vertical channels. The sub-geometries were chosen from the criterion that the noise should be uncorrelated between channels. Due to the wide response pattern of the incoherent beams (Ringdal et al, 1975), only one incoherent beam (with infinite velocity) was formed for each filter band.

4) For each filter band, form an incoherent beam from the eight horizontal channels.

5) Under the assumption that the SNR is lognormally distributed during noise conditions, it can be shown that the cumulative distribution of number of detections versus detection threshold, approximately follows a straight line when both are plotted with logarithmic axes (see Appendix 1). In this study, we have selected a time interval (1987/:072.04.30.0 - 1987/072:16.00.00.0), and run all beams with a low threshold. From the cumulative distributions we have extrapolated the noise slopes down to a common level, in this case 10 detections, and found the corresponding detection thresholds.

In addition to the obtained threshold values, a description of the beam deployment is given in Table VII.3.2a and Table VII.3.2b.

Fig. VII.3.1 (a-l) show the cumulative distributions for the coherent P-beams and the incoherent beams made from the vertical channels. The dashed tangent lines are the inferred noise slopes extrapolated down to the 10 detections level. At this threshold we thus expect to have 10 false alarms ("noise detections") in each filter band during the examined time interval.

From Fig. VII.3.1 we can see that the threshold differences between the coherent and incoherent beams vary between 4.5 and 7 decibels. From this observation we can infer that for detection of phases where we consistently can achieve coherent beam gain exceeding these threshold differences, coherent beam detection is superior to incoherent detection. From NORESS experience (Kværna and Mykkeltveit, 1986), coherent beamforming of Pn phases will typically result in a SNR gains between 8 and 15 dB, thus coherent beams are clearly superior for P-phase detection. For secondary phases like Lg where we may not achieve coherent beam gain exceeding the threshold differences, incoherent beamforming may outperform the coherent procedure.

Another interesting feature seen from Fig. VII.3.1i) and Fig. VII.3.1j), is the large number of detections exceeding the obtained thresholds for the two filters 8.0-16.0 Hz and 10.0-16.0 Hz. These filter bands have been subjected to additional detection analysis of a 24 hours time interval, where we found that the majority of the detections exceeding the obtained thresholds occurred during working hours. A viable hypothesis is therefore that most of these detections are due to nearby man-made activity.

Fig. VII.3.2 (a-d) show the cumulative distributions for the incoherent beams from both the vertical and horizontal channels. An interesting feature is that the inferred thresholds from the incoherent beams based on 8 horizontal channels, is not higher than the thresholds inferred from the incoherent beams based on 22 vertical channels. This observation suggests that incoherent beamforming on a mixture of horizontal channels more effectively reduces the noise variance than using vertical channels alone.

The number of noise detections (10) chosen as a common limit for each filter band in this study is of course rather arbitrary, and has been made mainly for the purpose of achieving a common basis for comparison. In practical operation, it may be desirable to operate at different false alarm rates, and the corresponding thresholds may easily be inferred, e.g., to reduce the number of detections in the 8.0-16.0 Hz filter band by a factor of two (Fig. VII.3.1i), the thresholds have to be raised by about 3 decibels.

It should be emphasized that the false alarms discussed in this paper are due to the stochastic nature of the noise, and that intervals with different noise characteristics (Fyen, 1986) may give deviations from these curves. Noise bursts and close events which may be considered as false alarms do not follow the lognormal distribution. To avoid detection of these signals, the thresholds would have to be raised above the levels obtained in this study. Fig. VII.3.3 shows a histogram of RONAPP detections with apparent velocities less than 3.0 km/s for a period of 86 days. These signals are mostly generated by local activity in the northeastern direction from NORESS. These detections can easily be separated from the 'interesting' local and regional events on the basis of their apparent velocities. The incoherent beams that mostly

detect these local events, are also our best tool for detecting regional Lg phases. So raising the threshold to avoid the low velocity signals, would also imply missing a number of regional Lg detections. This illustrates some of the conflicting interests that has to be taken into account when determining thresholds and detection beams.

In conclusion, the thresholds obtained from the extrapolated noise slopes, indicate the lowest operational level. If in the detection process we want to exclude signals generated by nearby activity or local noise bursts, the thresholds should be raised. But as outlined earlier, many other factors have to be considered for a final beam deployment and the corresponding thresholds.

T. Kværna
S. Kibsgaard
F. Ringdal

References

Fyen, J. (1986): NORESS noise spectral studies - noise level characteristics. Semiannual Technical Summary, 1 April - 30 September 1986, NORSAR Sci. Rep. No. 1-86/87, Kjeller, Norway.

Kværna, T. and S. Mykkeltveit (1986) Optimum beam deployment for NORESS P-wave detection. Semiannual Technical Summary, 1 April - 30 September 1986, NORSAR Sci. Rep. No. 1-86/87, Kjeller, Norway.

Ringdal. F., E.S. Husebye and A. Dahle (1975): P-wave envelope representation in event detection using array data, in Exploitation of Seismograph Networks, K. G. Beauchamp, Editor,

Appendix 1

We assume that the quantity STA/LTA (short-term to long-term average) computed at regular intervals on a seismic trace (beam or single channel) follows a lognormal distribution during noise conditions (Ringdal et al, 1975).

Setting U = log (STA/LTA) we thus get the following probability density of this variable

$$f(u) = \frac{1}{\sqrt{2\pi}\cdot\sigma} \cdot e^{-\frac{(u-\mu)^2}{2\sigma^2}} = \frac{1}{\sigma} \cdot \phi\left(\frac{u-\mu}{\sigma}\right) \qquad (1)$$

where $\phi(z)$ denotes the standard Gaussian density.

The probability of U exceeding a given threshold value becomes

$$F(u) = P(U \geq u) = \int_u^\infty f(t)\, dt = 1 - \Phi\left(\frac{u-\mu}{\sigma}\right) \qquad (2)$$

where $\Phi(z)$ denotes the standard Gaussian distribution function.

With a logarithmic frequency axis, we obtain from (2) the following slope S(u) of the distribution function at a given threshold u

$$S(u) = \frac{d(\log F(u))}{du} = \frac{F'(u)}{F(u)} = \frac{-\frac{1}{\sigma} \cdot \phi\left(\frac{u-\mu}{\sigma}\right)}{1 - \Phi\left(\frac{u-\mu}{\sigma}\right)} \qquad (3)$$

For values of $t \geq 3$, we may use the following approximation, with a relative error of less than 10 per cent:

$$1 - \Phi(t) \approx \frac{1}{t} \cdot \phi(t) \qquad (4)$$

Applying this approximation to (3), and also noting that $\mu \approx 0$, since STA/LTA fluctuates around 1 during noise conditions, we obtain

$$S(u) \approx -\frac{u}{\sigma^2} \qquad \text{for } \frac{u}{\sigma} \geq 3 \qquad (5)$$

In practical detector operation, we are only interested in thresholds corresponding to large values of $\frac{u}{\sigma}$, thus the approximation (5) is applicable. For example, a threshold value of $u = 3.5 \cdot \sigma$ corresponds to 1 false alarm in 4000 independent STA/LTA computations, whereas $u = 4\sigma$ gives 1 false alarm per 30,000 such computations. A practical operating threshold is likely to be somewhere between these values; thus the slope (5) will be approximately constant around the threshold value, for a given σ.

Nr.	Prototype	Type	Low	High	Order
BP01	BU	BP	1.0	3.0	3
BP02	BU	BP	1.5	3.5	3
BP03	BU	BP	2.0	4.0	3
BP04	BU	BP	2.5	4.5	3
BP05	BU	BP	3.0	5.0	3
BP06	BU	BP	3.5	5.5	3
BP07	BU	BP	5.0	7.0	3
BP08	BU	BP	6.5	8.5	3
BP09	BU	BP	8.0	16.0	3
BP10	BU	BP	10.0	16.0	3
BP11	BU	BP	1.0	2.0	2
BP12	BU	BP	2.0	3.0	2

Table VII.3.1 This table show the filters applied in the experiment. All were recursive Butterworth bandpass filters of order 2 or order 3.

Coherent P-Beams

Filter	Configuration	# beams	Test(dB)	Threshold(dB)	# Detections
1.0- 3.0 Hz	A0 CD	1	6.0	12.0	28
1.5- 3.5 Hz	A0 CD	1	6.0	11.0	40
2.0- 4.0 Hz	A0 CD	10	6.0	12.7	51
2.5- 4.5 Hz	A0 BCD	10	6.0	12.4	50
3.0- 5.0 Hz	A0 BC	7	6.0	11.4	58
3.5- 5.5 Hz	A0 BC	9	6.0	10.9	64
5.0- 7.0 Hz	A0 BC	9	6.0	11.7	64
6.5- 8.5 Hz	A0 BC	9	6.0	11.5	70
8.0-16.0 Hz	A0AB	8	4.0	8.4	100
10.0-16.0 Hz	A0AB	8	4.0	8.5	114
1.0- 2.0 Hz	A0 CD	1	6.0	12.7	29
2.0- 3.0 Hz	A0 CD	1	6.0	12.7	28

Coherent S-Beams

Filter	Configuration	# beams	Test(dB)	Threshold(dB)	# Detections
1.0- 3.0 Hz	A0 CD	6	6.0	12.7	40
1.5- 3.5 Hz	A0 CD	12	6.0	12.9	49
2.0- 4.0 Hz	A0 CD	12	6.0	12.9	58
2.5- 4.5 Hz	A0 BCD	12	6.0	12.5	66
3.0- 5.0 Hz	A0 BC	12	6.0	12.3	58
3.5- 5.5 Hz	A0 BC	12	6.0	12.0	61
5.0- 7.0 Hz	A0 BC	12	6.0	12.7	45
6.5- 8.5 Hz	A0ABC	12	6.0	11.8	72
8.0-16.0 Hz	A0AB	12	6.0	9.0	93
10.0-16.0 Hz	A0AB	12	6.0	9.0	114
1.0- 2.0 Hz	A0 CD	6	6.0	13.2	33
2.0- 3.0 Hz	A0 CD	12	6.0	13.7	49

Table VII.3.2a In addition to the inferred thresholds and the number of detections exceeding these thresholds, a description of the coherent beam deployment for detection of P and S-phases is shown in this table. The respective coloums describe the following parameters:

Filter : The investigated filter band.
Configuration: The array sub-geomery applied in the beamforming. A0 means A0Z, A means A-ring, etc.
beams : Number of coherent beams within the filter band.
Test : The experimental threshold in dB.
Threshold : The threshold in dB inferred form the slope of the cumulative distributions.
Detections : Number of detections exceeding the deduced thresholds.

Incoherent beams on vertical channels

Filter	Configuration	# beams	Test(dB)	Threshold(dB)	# Detections
1.0- 3.0 Hz	A0 CD	1	1.9	6.4	48
1.5- 3.5 Hz	A0 CD	1	1.9	6.6	61
2.0- 4.0 Hz	A0 CD	1	1.9	6.9	44
2.5- 4.5 Hz	A0 BCD	1	1.9	6.9	42
3.0- 5.0 Hz	A0 BCD	1	1.9	7.2	33
3.5- 5.5 Hz	A0 BCD	1	1.9	6.8	36
5.0- 7.0 Hz	A0 BCD	1	1.2	4.7	72
6.5- 8.5 Hz	A0 BCD	1	1.2	4.5	95
8.0-16.0 Hz	A0 BCD	1	1.2	4.0	77
10.0-16.0 Hz	A0 BCD	1	1.2	4.0	80
1.0- 2.0 Hz	A0 CD	1	1.9	6.8	36
2.0- 3.0 Hz	A0 CD	1	1.9	7.9	45

Incoherent beams on horizontal channels

Filter	Configuration	# beams	Test(dB)	Threshold(dB)	# Detections
1.0- 3.0 Hz	E-W N-S	1	1.9	6.8	35
1.5- 3.5 Hz	E-W N-S	1	1.9	7.0	50
2.0- 4.0 Hz	E-W N-S	1	1.9	7.4	40
2.5- 4.5 Hz	E-W N-S	1	1.9	6.8	48
3.0- 5.0 Hz	E-W N-S	1	1.9	6.1	54
3.5- 5.5 Hz	E-W N-S	1	1.9	5.3	52
5.0- 7.0 Hz	E-W N-S	1	1.2	5.1	44
6.5- 8.5 Hz	E-W N-S	1	1.2	4.8	81
8.0-16.0 Hz	E-W N-S	1	1.2	3.7	81
10.0-16.0 Hz	E-W N-S	1	1.2	3.7	92
1.0- 2.0 Hz	E-W N-S	1	1.9	7.3	23
2.0- 3.0 Hz	E-W N-S	1	1.9	8.6	29

Table VII.3.2b In this table we have shown the same parameters as in Table VII.3.2a, but now for the incoherent beams. E-W means the channels A0E, C2E, C4E and C7E. N-S means the channels A0N, C2N, C4N and C7N.

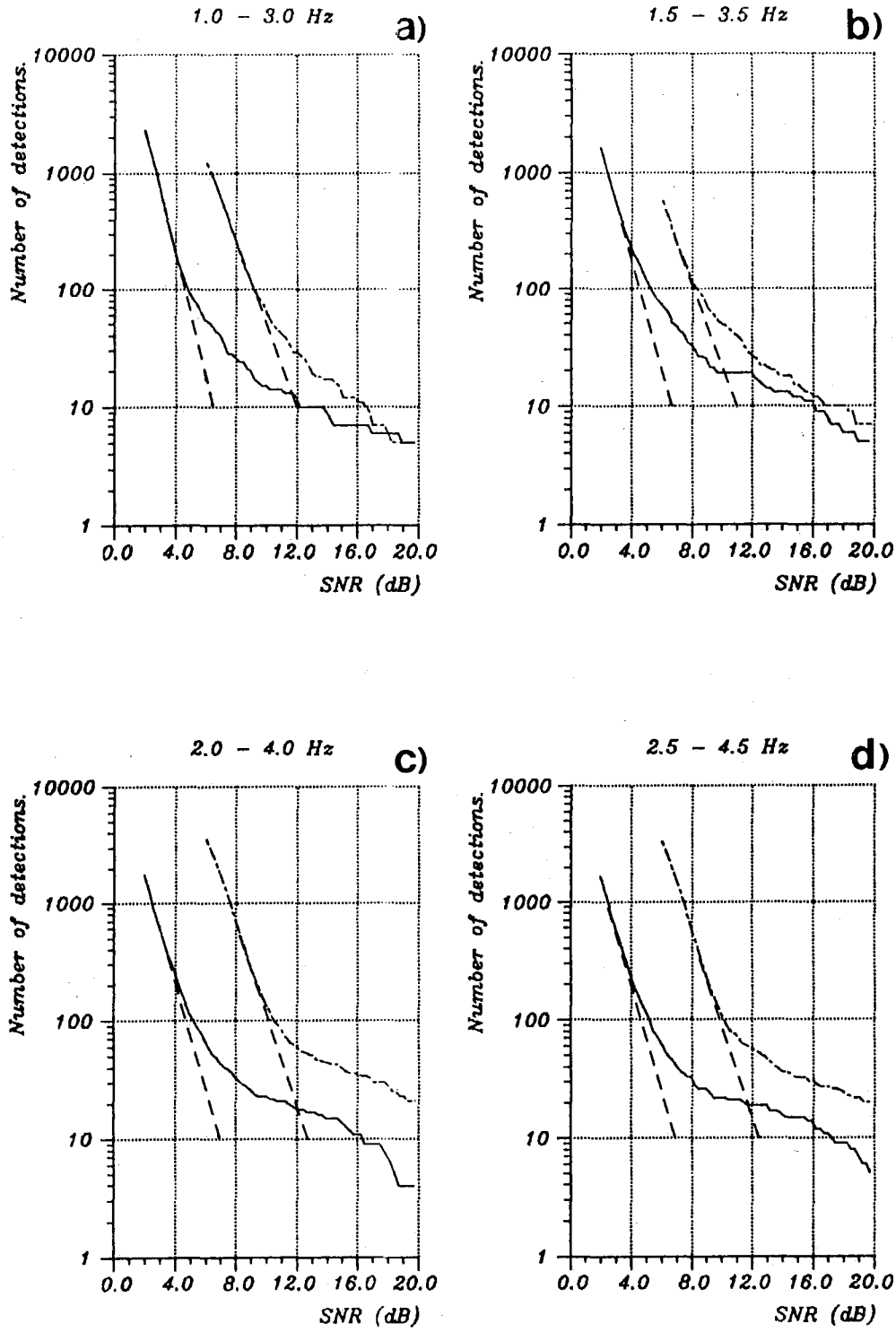

Fig. VII.3.1 These figures (a-1) show the cumulative distributions for the coherent P-beams (dashed-dotted curves) and for the incoherent beams made from the vertical channels (solid lines) in all filter bands investigated. The dashed lines indicate the slopes of the distribution of 'noise' detections.

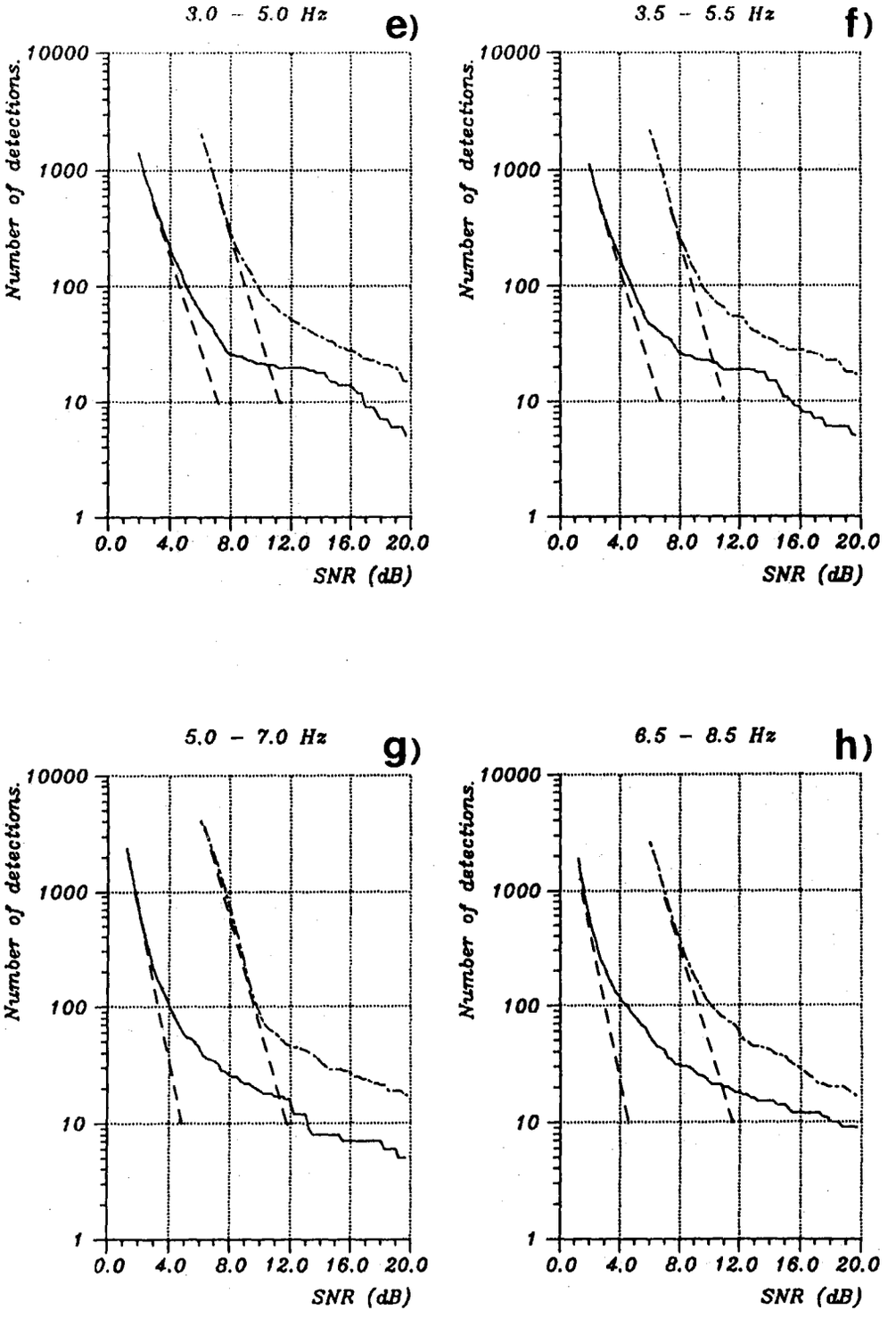

Fig. VII.3.1 (cont.)

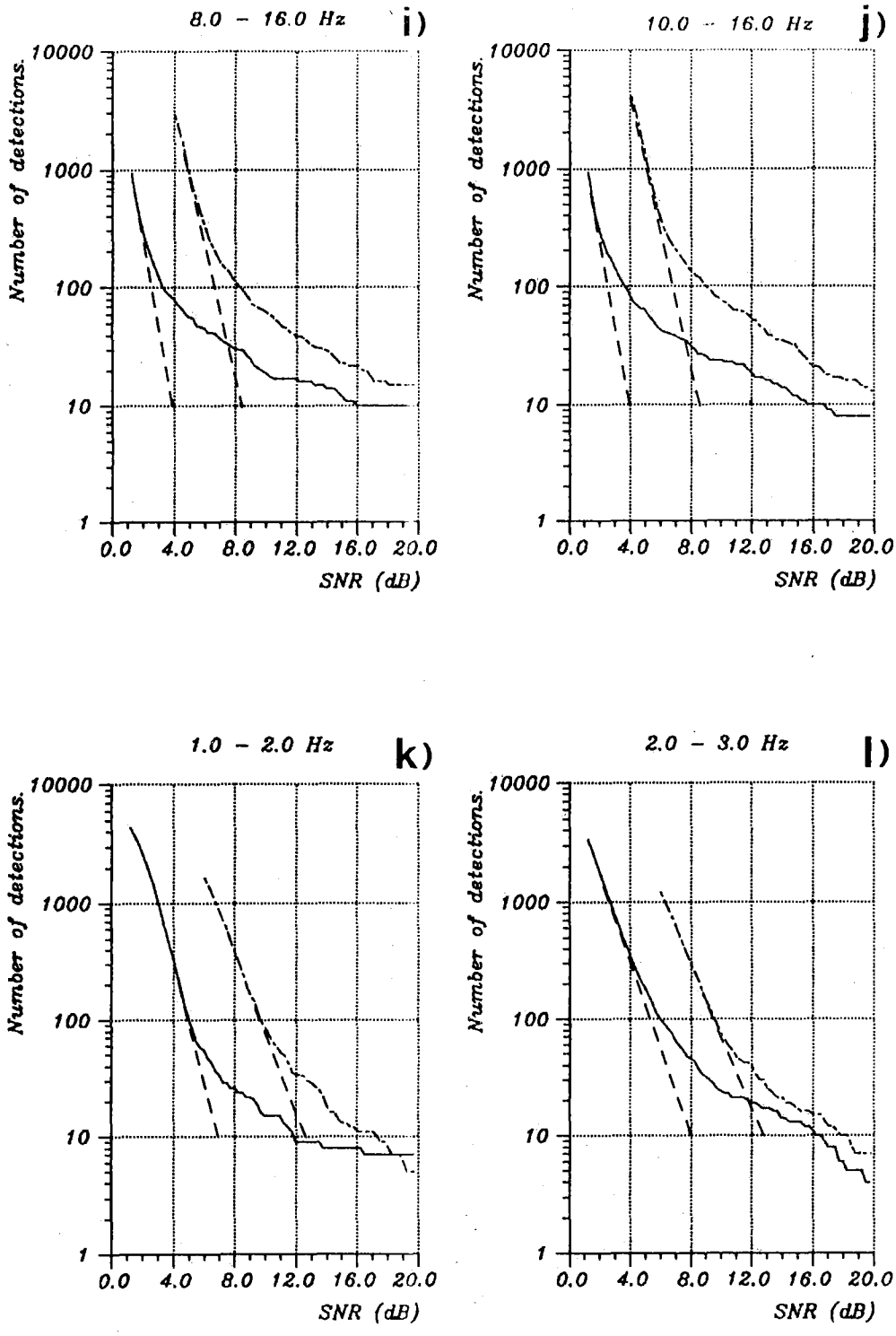

Fig. VII.3.1 (cont.)

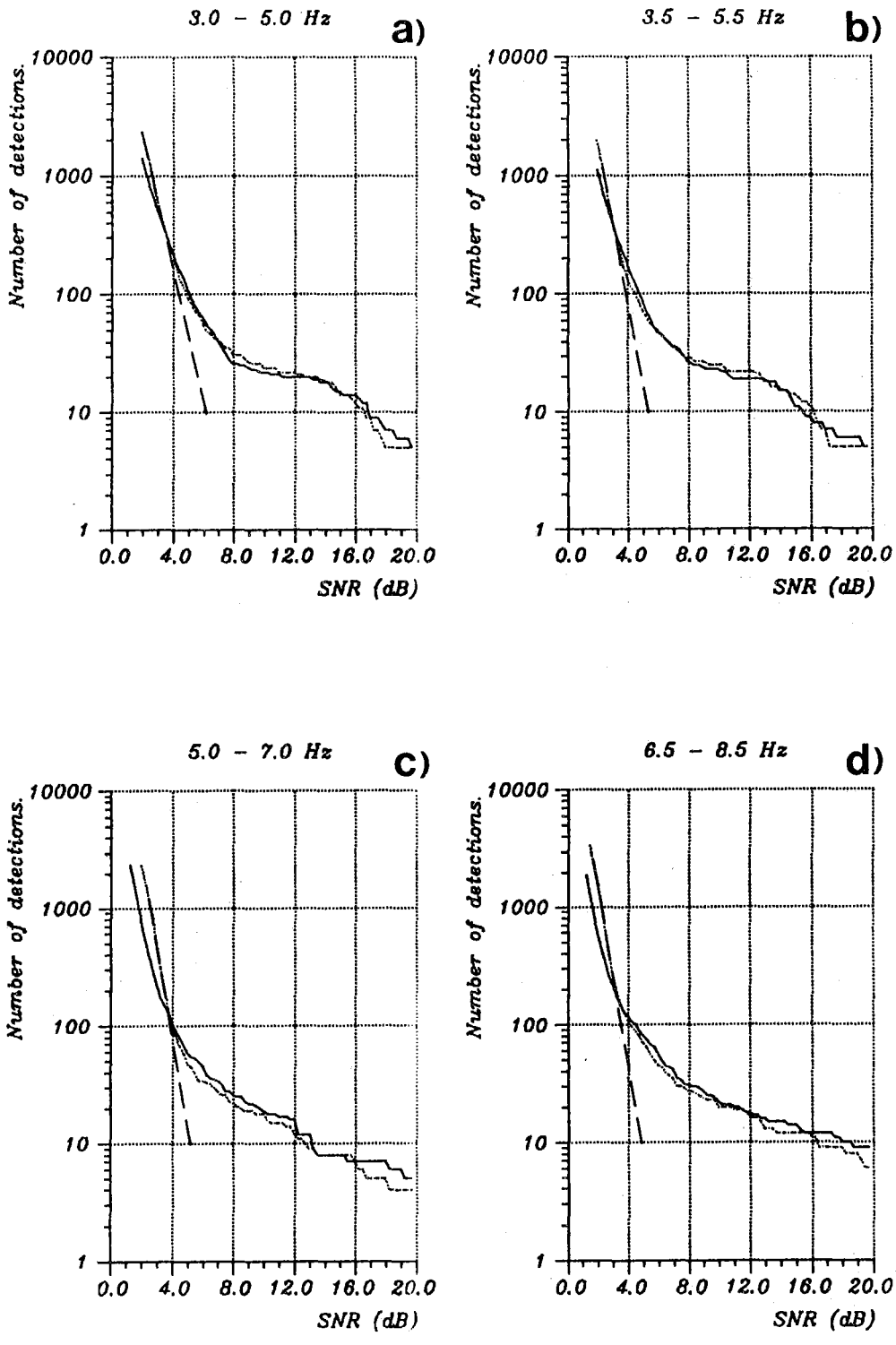

Fig. VII.3.2 This figure (a-d) show the cumulative distributions for the incoherent beams from the vertical channels (solid lines) and from the horizontal channels (dotted lines) for four different filter bands. The dashed lines indicate the noise slopes inferred from the 'noise' distributions of the 'horizontal' beams.

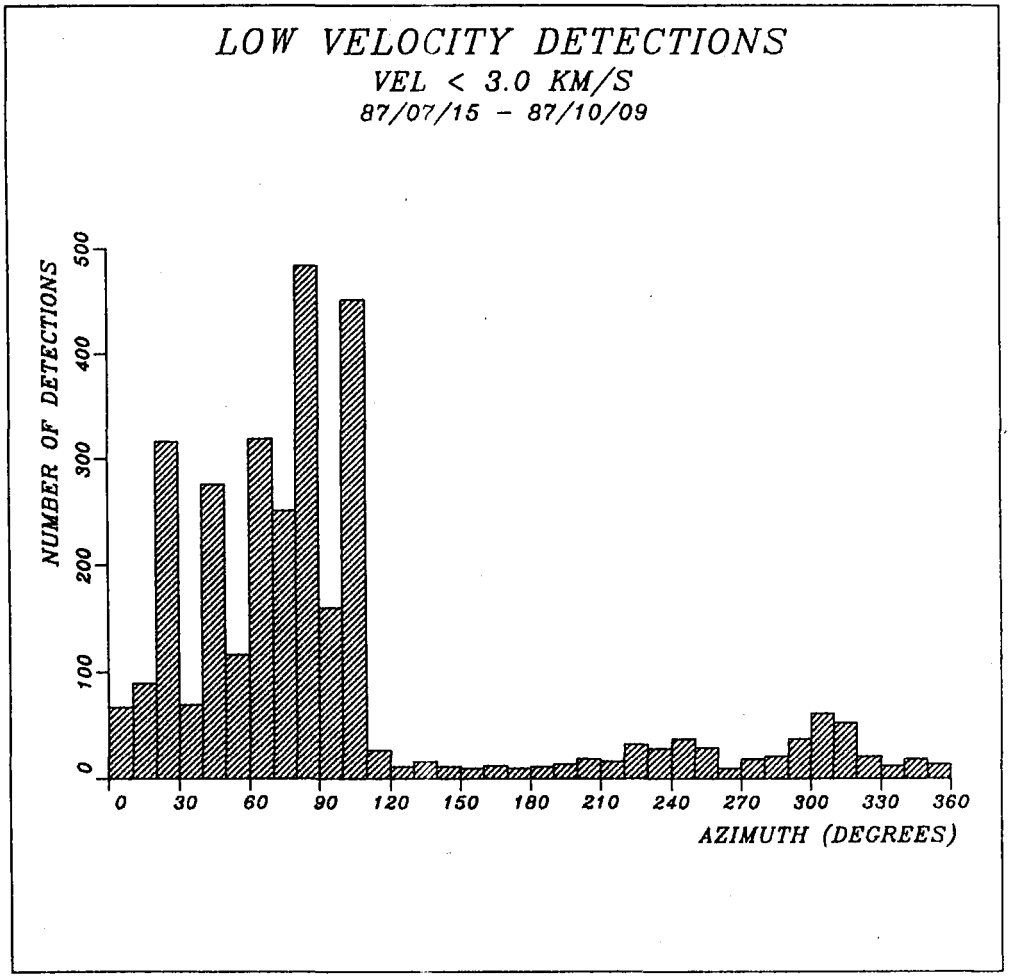

Fig. VII.3.3 This histogram displays the azimuthal distribution of RONAPP detections during the 86-day period indicated, with apparent velocities less than 3.0 km/s. Within the investigated time interval there were totally 10000 detections. 3140 of these detections had an apparent velocity less than 3.0 km/s.